Journal of
Materials Chemistry B

Accepted Manuscript

This article can be cited before page numbers have been issued, to do this please use: Q. Li, J. Cao, Q. Wang, J. Zhang, S. Zhu, Z. Guo and W. Zhu, *J. Mater. Chem. B*, 2019, DOI: 10.1039/C8TB03188F.

ROYAL SOCIETY OF CHEMISTRY

rsc.li/materials-b

ROYAL SOCIETY OF CHEMISTRY
View Article Online
DOI: 10.1039/C8TB03188F

Journal Name

ARTICLE

Nanomized tumor-microenvironment active NIR fluorescent prodrug for ensuring synchronous occurrences of drug releasing and fluorescence tracing†

Received 00th January 20xx,
Accepted 00th January 20xx

DOI: 10.1039/x0xx00000x

www.rsc.org/

Qiang Li,[a] Jun Cao,[b] Qi Wang,*[,a] Jie Zhang,[a] Shiqin Zhu,[a] Zhiqian Guo[a] and Wei-Hong Zhu*[,a]

Improving the prodrug bioavailability and tumor targeting ability, as well as monitoring active ingredient release *in vivo*, is still a challenge for cancer diagnosis and therapy. Herein, a specific nanomized tumor-microenvironment active near-infrared (NIR) fluorescent prodrug DCM-S-GEM/PEG as a potent monitoring platform is developed, in which we conjugate antitumor drug gemcitabine (GEM) and the NIR fluorescent chromophore dicyanomethylene-4*H*-pyran (DCM) *via* a glutathione (GSH) activatable disulfide linker, and encapsulate DCM-S-GEM into the amphiphilic polymer DSPE-mPEG by self-assembling. The nanomized prodrug DCM-S-GEM/PEG exhibits excellent photostability and high biocompatibility, significantly improving the therapeutic efficacy to lung tumor cells with low side effects to normal cells. Furthermore, compared with the free prodrug DCM-S-GEM, the micelliazation with diblock DSPE-mPEG avoids fast metabolism, facilitates the accumulation of drugs in lung tumor tissues, displays longer tumor retention, and realizes precise drug release in lung tumor. The nanomized DCM-S-GEM/PEG can be developed as a promising tool to monitor prodrug delivery and activation process *in vivo*.

Introduction

Chemotherapy is an indispensable choice for most cancer cases because of its high efficiency among various cancer treatments.[1] Conventional chemotherapy suffers from poor bioavailability because of the rapid blood clearance, and nonspecific selectivity along with low accumulation in tumors.[2,3] To address these limitations, prodrugs are widely used in the chemotherapies,[4] such as peptide-based prodrugs[5] for improving tumor targeting ability, amino acid-based prodrugs[6] for enhancing both tumor targeting ability and solubility, aptamer–based[7] prodrugs for higher specificity as well as affinity, and enzyme cleavable[8] or activated[9] prodrugs for high specificity and enhanced therapy. Unfortunately, restricted by the small size, free anti-cancer prodrug still faces the challenges of fast clearance by blood or kidney, poor bioavailability, adverse therapeutic effects, especially huge unpredictability, which greatly limit the clinical application.[10] Therefore, a strategy for improving the bioavailability and tumor targeting ability, as well as monitoring active ingredient release from prodrug is urgently required in tumor therapy.

Fluorophores-labelled prodrugs are helpful for monitoring the release and eliminating the unpredictability of chemotherapeutic agent by precise pharmacodynamics evaluation. It is advantageous of individualized treatment as well as low toxicity, non-invasive properties and forceful compliance.[11,12] However, the long-real-time drug tracing *in vivo* is still a huge challenge, owing to the inaccuracy, instability, and the systematic toxicity in the intricate internal environment.[13] Whereas, polymeric micelle,[14] whose nanoscopic structure was formed through the self-assembly of amphiphilic copolymer, is helpful for improving the tumor targeting, regulating the bioavailability as well as increasing stability of prodrug or fluorescent sensors. As reported, polymeric micelle exhibits good biodegradability,[15] stability,[16] targeting property,[17] water dispersibility,[18] and selectivity,[19] further facilitates blood circulation of the prodrug vesicles by suppressing protein absorption and avoiding recognition with macrophages.[20]

Hence, in this work, we design a nanomized tumor-microenvironment active near-infrared (NIR) prodrug DCM-S-GEM/PEG to trace the drug fate and improve the bioavailability *in vivo* owing to the following considerations (Fig. 1A): i) the DSPE-mPEG micelles[21,22] encapsulate the prodrug DCM-S-GEM, ensuring both high water dispersity, tumor targeting, and long time retention along with low side toxicity, ii) the fluorophore dicyanomethylene-4*H*-pyran (DCM) chromophore[23-26] ensures the long-time low-toxic tracing because of the excellent emission ability, high photostability and NIR region, iii) the disulfide bond (-S-S-) is specifically cleavable by tumor-overexpressed glutathione (GSH) which ensures the tumor targeting and negative systematic toxicity,[27-29] and chemotherapeutic agent gemcitabine (GEM)[30-32] is connected to fluorophore DCM, which ensures the synchronous occurrences of the drug releasing and fluorescence lighting. The tumor-environment active prodrug DCM-S-GEM/PEG exhibited high toxicity to tumor cells, low side effects to normal cells, strong photostability, and excellent sensitivity in both live A549 cells and lung cancer mice model, providing an potential approach to real-time and long-time monitoring of the drug delivery and activation process *in vivo*.

[a] *Shanghai Key Laboratory of Functional Materials Chemistry, Key Laboratory for Advanced Materials and Institute of Fine Chemicals, Joint International Research Laboratory of Precision Chemistry and Molecular Engineering, Feringa Nobel Prize Scientist Joint Research Center, School of Chemistry and Molecular Engineering, East China University of Science and Technology, Shanghai 200237, China. *E-mail: wangqi@ecust.edu.cn, whzhu@ecust.edu.cn*

[b] *Department of Interventional Oncology, Dahua Hospital, Xuhui District, Shanghai 200237, China.*

†*Electronic supplementary information (ESI) available: Reagents and instruments, synthetic procedures, ^{1}H and ^{13}C NMR, and HRMS information. See DOI: 10.1039/x0xx00000x*

View Article Online
DOI: 10.1039/C8TB03188F

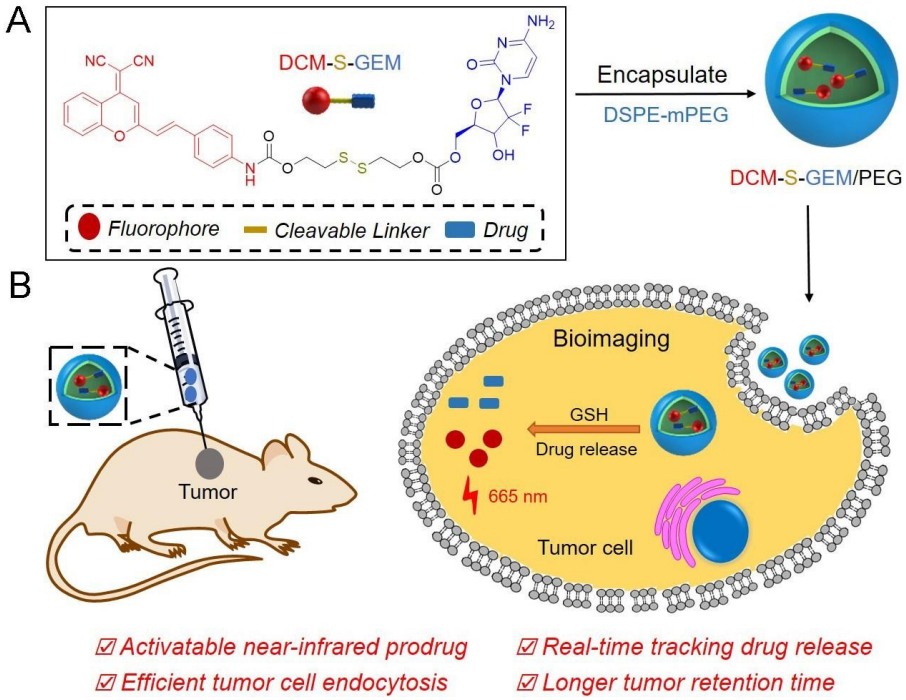

Fig. 1 Tumor-microenvironment active NIR fluorescent platform DCM-S-GEM/PEG for tumor therapy and drug monitoring. (A) The tumor-microenvironment sensitive fluorescent platform DCM-S-GEM/PEG generated by assembling the prodrug DCM-S-GEM into the DSPE-mPEG micelles. (B) Tumor treatment is conducted that, i) injecting the DCM-S-GEM/PEG into the tumor tissue, ii) the DCM-S-GEM/PEG is internalized, and followed by iii) selectively cleavage of prodrug and light up of fluorescence.

Results and discussion

Micellizing fluorescent prodrug for solving its bioavailability and tumor targeting ability

GEM, a DNA chain terminator, is one of the widely used agents in the treatment for several solid tumors, especially for non-small-cell lung cancer.[33,34] GEM provides an improvement in the quality of life, but the side effects and acquired drug resistance seriously limit its clinical efficacy.[35,36] Here, a fluorescent prodrug DCM-S-GEM was designed and synthesized to reduce the side effects, improve the tumor targeting ability and trace the accurate drug distribution. Briefly, compounds DCM, DCM-NH_2 and DCM-S were synthesized according to the previous work,[27,37] and the final product DCM-S-GEM was obtained by mixing DCM-S and GEM in the presence of triphosgene at room temperature followed by stirring. All intermediates and final product DCM-S-GEM were characterized using ^1H, ^{13}C NMR, and high-resolution mass spectrometry (HRMS, Fig. S1-S9 in ESI†). The chemical structure of DCM-S-GEM was described in Fig. 1A that, i) DCM chromophore with controllable emission, high fluorescent brightness, and strong photostability ensuring the satisfying tissue penetration and long time fluorescence imaging in cells, ii) GEM, a first line chemotherapeutic agent for non-small-cell lung cancer treatment, iii) disulfide bond, the tumor-environment active linker between DCM derivative and GEM, ensuring the selectively cleavage in tumor tissue for eliminating the side effects and tracing the drug release. Then, DCM-S-GEM was encapsulated into diblock polymer DSPE-mPEG (abbreviated as DCM-S-GEM/PEG), a amphiphilic polymer drug carrier with superior biocompatibility, to improve the aqueous dispersibility, avoid the fast clearance, regulate biocompatibility and further enhance the cellular internalization as well as extend retention time in tumor tissue (Fig. 1B).[38,39]

GSH-active response of fluorescent prodrug DCM-S-GEM

The disulfide bond is a well-known activatable linker by thiols, such as GSH, Cys, Hcy, and so on.[27,28,40] Since the tumor cells express much more GSH with respect to normal cells,[41-43] the fluorescent prodrug DCM-S-GEM is proposed to be selectively cleaved in tumor tissue, followed by releasing NIR fluorescence chromophore DCM for tumor imaging as well as drug tracing, and chemotherapeutic agent GEM for cancer treatment.

In order to demonstrate whether the fluorophore of DCM and chemotherapeutic agent of GEM can be concomitantly released from the disulfide bond-linked prodrug DCM-S-GEM, HPLC spectra analysis and mass spectroscopy are carried out by incubating DCM-S-GEM with biologically available thiols GSH. As illustrated in Fig. 2B, the prodrug DCM-S-GEM, fluorophore DCM-NH_2, and the antitumor drug GEM showed narrow peaks with retention time at 16.4, 4.7 and 7.9 min, respectively. After incubating the prodrug DCM-S-GEM with GSH for 30 min, a new sharp peak at 4.7 min corresponding to DCM-NH_2, a narrow peak at 7.9 min for GEM and a decreased peak corresponding to DCM-S-GEM at 16.4 min appeared, indicating the DCM-S-GEM was cleaved by GSH. Also, after incubating for 20 min, the mixture were analyzed by mass spectroscopy, showing three *m/z* peaks 264.0756, 312.0879, and 781.2097 associated with [GEM + H^+] (calcd. 264.0790 for $C_9H_{12}F_2N_3O_4^+$), [DCM-NH_2 + H^+] (calcd. 312.1131 for $C_{20}H_{14}N_3O^+$) and [DCM-S-GEM + H^+] (calcd.781.1557 for $C_{35}H_{31}F_2N_6O_9S_2^+$) (Fig. S10†). Both experiments demonstrated the fluorescent prodrug DCM-S-GEM is cleaved by GSH, followed by releasing pharmaceutical agent GEM and fluorescence agent DCM-NH_2 (Fig. 2A).

View Article Online
DOI: 10.1039/C8TB03188F

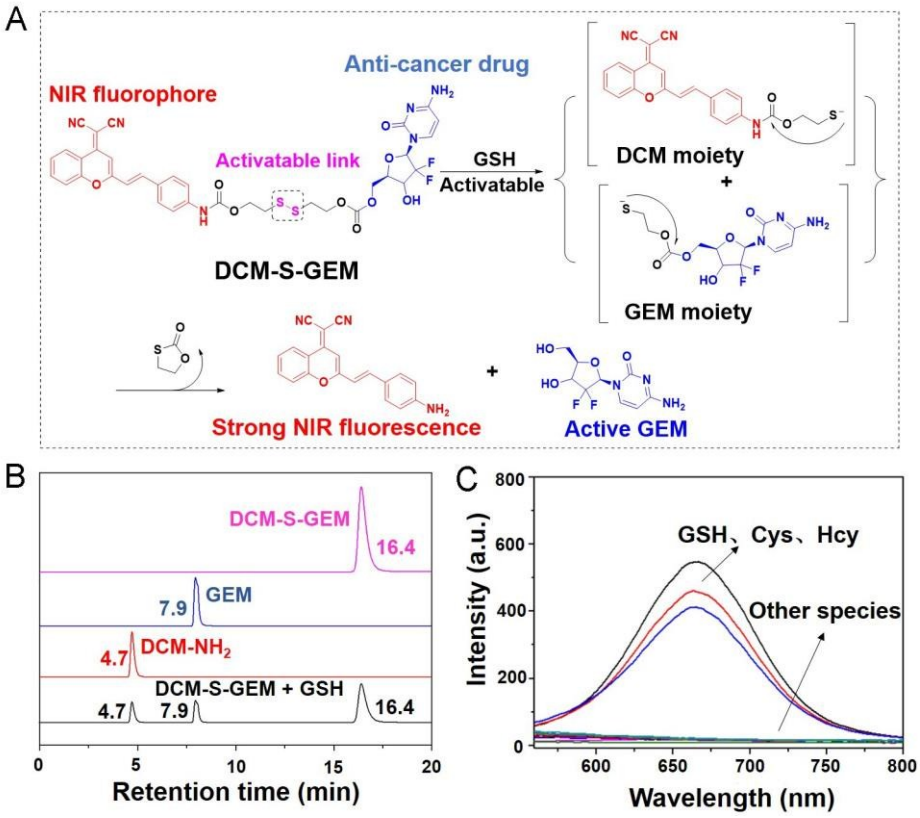

Fig. 2 GSH-activatable response of fluorescence prodrug DCM-S-GEM. (A) Response mechanism of DCM-S-GEM with GSH under physiological conditions for drug release, in which the disulfide bond (-S-S-) can be cleaved via GSH. (B) HPLC spectra of DCM-S-GEM, GEM, DCM-NH_2, and reaction product of DCM-S-GEM incubated with 2.5 mM GSH for 50 min. (C) Fluorescence spectra and (D) fluorescence intensity (665 nm) towards various amino acids including GSH, Cys, Hcy, Ala, Arg, Asn, Asp, Gln, Glu, Gly, His, Ile, Leu, Phe, Pro, Ser, Thr, Tho, Tyr, Val, respectively (50 μM). Note: Fluorescence enhancement was observed in thiol-treatment groups, indicating excellent selectivity to thiol of DCM-S-GEM.

High selectivity is essential for high efficiency as well as low side toxicity in cancer treatment.[44-46] Hence, the specificity of the NIR fluorescent prodrug DCM-S-GEM toward GSH was performed. Various potential interfere species were tested in this experiment to verify the specificity of DCM-S-GEM, including enzyme species, amino acids, and so on. As shown in Fig. 2C, the fluorescence intensity of DCM-S-GEM was much higher in thiol-containing amino acids (glutathione, cysteine and homocysteine) than non-thiol-bearing amino acids, indicative of excellent specificity to thiol-containing amino acids. Actually, the potential interference of Cys and Hcy can be neglected due to their relatively low concentration compared to the high physiological concentration of GSH in the cytoplasm.[23] Considering with the much higher GSH concentration in tumor cells to normal cells, this prodrug is supposed with tumor targeting ability. As demonstrated, the fluorescent prodrug DCM-S-GEM can be specially cleaved by GSH (tumor highly expressed), ensuring the tumor target ability along with limiting side effects.

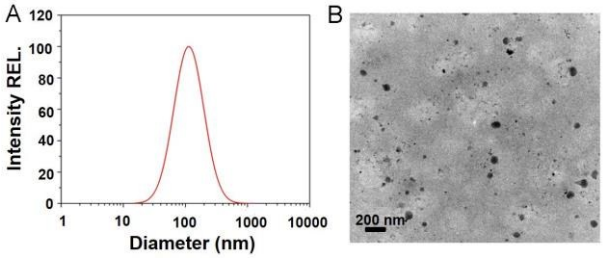

Fig. 3 Characterization of DCM-S-GEM/PEG micelles *via* (A) transmission electron microscopy (TEM) and (B) dynamic light scattering (DLS). The size of DCM-S-GEM/PEG is 110 nm with PDI of 0.192.

"Turn on" fluorescent property of nanomized prodrug DCM-S-GEM/PEG for drug release monitoring

As shown in Fig. 3, DCM-S-GEM/PEG was well-organized of 110 nm (PDI 0.192) with good morphology and dispersity (Fig. 3), and drug loading effect of 5.21% (Fig. S11†), suggestive of high enhanced permeability and retention (EPR) effect and low side effects. Owing to the NIR fluorescent probe for tissue penetrating, the tumor-environment active disulfide bond for drug tracing, and the micelle structure for superior biocompatibility and tumor targeting ability, as well as extended tumor retention, the nanomized tumor-microenvironment active NIR DCM-S-GEM/PEG is excepted to realize real-time drug release monitoring and improved tumor lethality.

As demonstrated, the prodrug DCM-S-GEM can be cleaved by GSH into fluorophore DCM and drug GEM. In order to further study the fluorescent property, the UV-Vis absorption and fluorescence

View Article Online
DOI: 10.1039/C8TB03188F

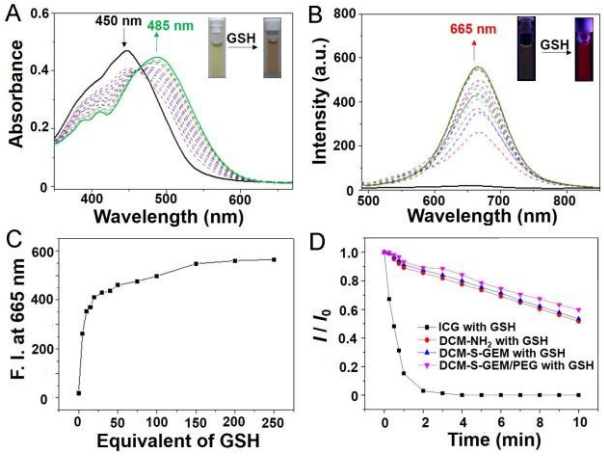

Fig. 4. Tumor-microenvironment sensitive fluorescence 'turn on' prodrug DCM-S-GEM with satisfying photostability. Absorption (A) and emission spectra (B, λ_{ex} = 450 nm) of DCM-S-GEM (10 μM) in aqueous solution (DMSO/PBS = 1/1, v/v; pH = 7.4; 37 °C) upon treatment with increasing concentrations of GSH (0-250 equiv). Photo-image (inset A) and fluorescence-image (inset B) of DCM-S-GEM solution before and after addition of GSH. (C) Fluorescence enhancement at 665 nm with increasing GSH concentration. (D) Time-dependent fluorescence intensity of ICG (10 μM in DMSO/PBS = 1:1, treated with 2.5 mM GSH, monitored at 812 nm, and excited at 780 nm), DCM-NH_2, DCM-S-GEM and DCM-S-GEM/PEG (10 μM in DMSO/PBS = 1:1, treated with 2.5 mM GSH for 1 h at 37 °C, monitored at 665 nm and excited at 450 nm).

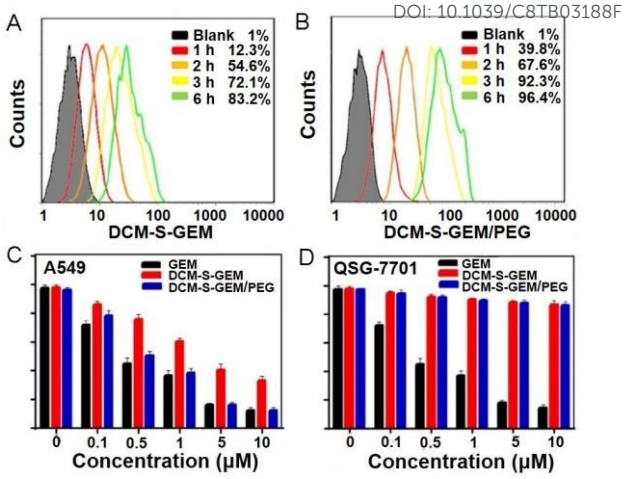

Fig. 5 Internalization and cytotoxicity of DCM-S-GEM/PEG to lung tumor cells (A549 cells) and normal cells (QSG-7701cells). Flow cytometry analysis of cellular uptake of (A) DCM-S-GEM and (B) DCM-S-GEM/PEG at different time intervals from 1 to 4 h in A549 cells. Cell viability of GEM, DCM-S-GEM, DCM-S-GEM/PEG to (C) QSG-7701 cells and (D) A549 cells. Note: DCM-S-GEM/PEG markedly facilitated cellular internalization in tumor cells and exhibited high cytotoxicity to A549 cells along with low cytotoxicity to QSG-7701 cells *in vitro*.

spectra were detected by incubating the prodrug DCM-S-GEM with biologically available thiols such as GSH (0-250 equiv). As shown in Fig. 4A, UV absorption gradually red shifted from 450 nm to 485 nm with an increased GSH concentration, along with a color turning from pale yellow to pink (inset of Fig. 4A). Also, the fluorescence intensity at 665 nm became increased after incubating with GSH (Fig. 4B and 4C), exhibiting 'turn-on' fluorescent characteristic, suggestive of precise bioimaging possibility of drug release in tumor tissue and biodistribution *in vivo*.

The photostability of NIR fluorophores is a significant portion for practical application especially in bioimaging.[47,48] Hence, the time-dependent fluorescence intensity of DCM-S-GEM and nanomized prodrug DCM-S-GEM/PEG were detected after GSH incubation. As shown in Fig. 4D and Fig. S12†, after exposure to high density light (Hamamatsu, LC8 Lightningcure, 300 W), the fluorescence intensity of the cyanine dye ICG (FDA-approved NIR contrast agent) decreased almost to vanishing point after 3 min, suggesting photobleaching vulnerability. In contrast, nearly 50% florescence of DCM-S-GEM/PEG and DCM-S-GEM were maintained after 10 min, indicative of higher photostability. Consequently, the DCM-S-GEM/PEG and DCM-S-GEM guarantee long-time tracing of chemotherapeutic agent *in vivo*. Taken together, the nanomized NIR fluorescent prodrug DCM-S-GEM/PEG is specially 'turn on' in tumor site with strong photostability, ensuring the precise and long time tumor imaging.

Enhanced treatment effect of DCM-S-GEM/PEG on lung tumor cells (A549 cells) *in vitro*

The intracellular drug concentration of chemotherapeutic drug can be used to predict the treatment effect. Hence, the internalization of DCM-S-GEM/PEG by lung cancer cells A549 was quantitatively detected through flow cytometry. As shown in Fig. 5, the fluorescence cells percent increased on a time-dependent manner for both DCM-S-GEM/PEG and DCM-S-GEM. Moreover, the DSPE-mPEG micelles improved the internalization that, the fluorescence percent is 39.6% for DCM-S-GEM/PEG at 1 h and 92.3% at 6 h (Fig. 5B) , compared to 12.3% at 1 h and 83.2% at 6 h for DCM-S-GEM (Fig. 5A), suggesting stronger treatment effect toward lung cancer cells.

Standard MTT assay was conducted to investigate the cytotoxicity of DCM-S-GEM/PEG against lung cancer cells A549. As illustrated in Fig. 5C, all GEM, DCM-S-GEM, and DCM-S-GEM/PEG showed obvious cytotoxicity to A549 cells at a concentration-dependent manner, with the half-maximal inhibitory concentration (IC_{50}) values of 0.443, 0.511 and 0.465 μM, respectively. Furthermore, limited by the poor solubility and biocompatibility, the small molecular prodrug DCM-S-GEM cannot guarantee a satisfactory treatment efficiency compared with free GEM. In contrast, owing to the good water dispersity and excellent biocompatibility, the cell viability of nanomized DCM-S-GEM/PEG is comparable with the free drug GEM. Obviously, both DCM-S-GEM and DCM-S-GEM/PEG are low toxic to QSG-7701 because of the low GSH concentration in normal cells compared with the strong cytotoxicity of free GEM, indicating negative side effects (Fig. 5D). The tumor-microenvironment sensitive disulfide linker and improved solubility guaranteed high cytotoxicity of DCM-S-GEM/PEG to cancer cells and low toxicity to normal cells.

The apoptosis property of DCM-S-GEM/PEG was detected using typical flow cytometry (FCM) analysis with Annexin V-FITC/PI double staining. The results showed that the percentage of cells with phosphatidylserine externalization (the typical characteristics of apoptosis) significantly increased in all GEM, DCM-S-GEM and DCM-S-GEM/PEG groups compared to control group. As illustrated in Fig. S13†, the apoptosis ratio increased in a concentration dependent manner that, the number are 8.00%, 26.5%, 50.0% and 64.7% after

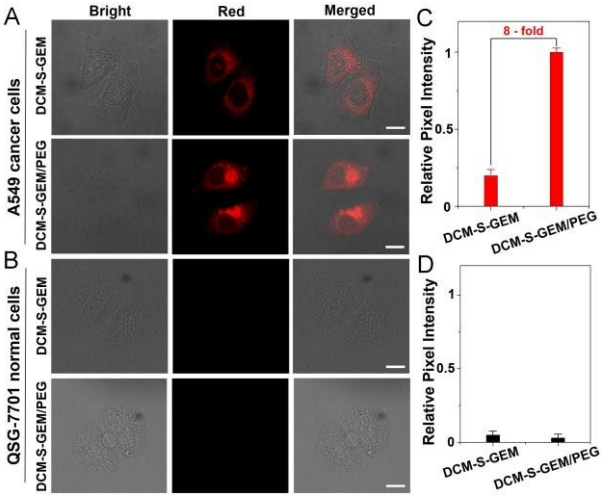

Fig. 6 Fluorescence images of cancer cells (A549 cells, A) and normal cells (QSG-7701 cells, B) with the incubation of DCM-S-GEM and DCM-S-GEM/PEG (10 μM) for 3 h, respectively. Red channel (DCM-NH_2) were obtained with excitation at 485 nm and a long-path (630-690 nm) emission filter. The relative pixel intensity of DCM-S-GEM and DCM-S-GEM/PEG in (C) tumor cells (A549 cells) and (D) normal cells (QSG-7701cells). All images share the same scale bar (30 μm). Note: The DCM-S-GEM/PEG can real-time trace the drug release and realize tumor diagnose.

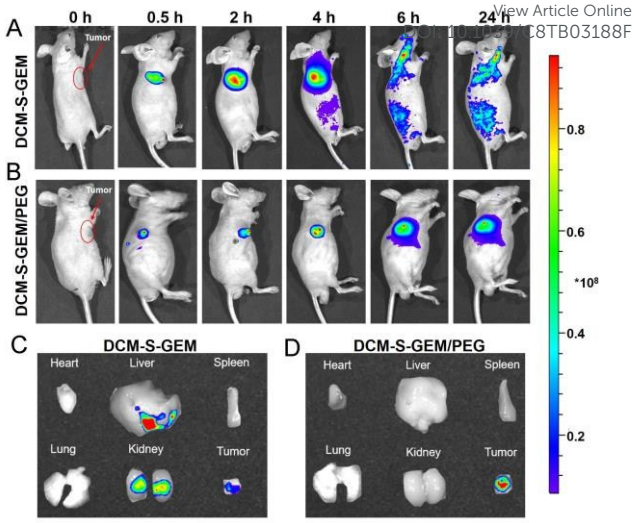

Fig. 7 Bioimaging of tumor-bearing mice at various time (0, 0.5, 2, 4, 6, 24 h) after orthotopic injection of (A) DCM-S-GEM and (B) DCM-S-GEM/PEG. *Ex vivo* images of major organs of mice after injection of (C) DCM-S-GEM and (D) DCM-S-GEM/PEG for 24 h. The color bars corresponding to the detected fluorescence intensity. Note: The tumor-microenvironment activable DCM-S-GEM/PEG is suitable for real-time tracing drug release *in vivo*.

treating with 0, 0.5, 1, 5 μM GEM for 48 h, respectively. Similarly, the apoptosis number are 21.2% (0.5 μM), 30.1% (1 μM) and 48.0% (5 μM) for DCM-S-GEM group, respectively. Limited by the cleavage rate between the DCM and GEM, the apoptosis ratio of small prodrug DCM-S-GEM was smaller than free GEM. Notably, the DCM-S-GEM/PEG induced the comparable apoptosis ratio to unbounded GEM at the concentration of 1 μM (56.2%) and 5 μM (63.0%), which are much higher apoptosis ratio at the concentration of 0.5 μM (43.2%, Fig. S14†). The DCM-S-GEM/PEG induced more cell apoptosis than free GEM because of the stronger internalization. Compared to the free GEM and prodrug DCM-S-GEM, the nanomized prodrug DCM-S-GEM/PEG has higher internalization and toxicity to tumor cells, owing to the good aqueous dispersity, excellent biocompatibility and the micelle structure, suggesting improved medicine efficiency.

Real-time monitoring of drug release in lung cancer cells

Due to the extraordinary internalization and GSH cleavable ability of DCM-S-GEM/PEG in tumor cells, the selectively lighting up of tumor tissues and drug tracing are proposed through releasing DCM in tumor-microenvironment. Hence, the fluorescence images of cancer cells (A549 cells) and normal cells (QSG-7701 cells) are obtained after incubation of DCM-S-GEM/PEG to evaluate the drug release visualization and tumor diagnosis. As shown in Fig. 6, the tumor cells A549 became lighted on upon incubation with either DCM-S-GEM or DCM-S-GEM/PEG (Fig. 6A) for 3 h. It is noted that, the nanomized prodrug DCM-S-GEM/PEG exhibited 8-fold stronger fluorescence intensity than prodrug DCM-S-GEM owing to the better water dispersity, higher biocompatibility, and stronger internalization (Fig. 6C). In contrast to tumor cells, the fluorescence is neglected in normal cells QSG-7701 (Fig. 6B and 6D) due to the low GSH concentration, suggesting precise drug releasing and real-time tracing as well as tumor diagnosis. As a result, the DCM-S-GEM/PEG platform can selectively lighting the tumor cells compared to the normal cells as well as labeling the drug releasing, suggesting a good tumor diagnosis and biodistribution evaluation probe.

Long-time and real-time monitoring of drug release in lung xenograft tumor model

As demonstrated in cell experiments, the nanomized DCM-S-GEM/PEG is highly internalized by lung tumor cells and cleaved by GSH in tumor cells, followed by fluorescence 'turn on' so as to trace the drug release. Herein, the DCM-S-GEM and DCM-S-GEM/PEG were orthotropic injected into the lung xenograft tumor of mice model and monitored the fluorescence for 24 h to evaluate the drug tracing ability *in vivo*.

As illustrated in Fig. 7, no fluorescence was observed in both DCM-S-GEM and DCM-S-GEM/PEG at 0 h post injection, suggesting no release of free drug GEM or fluorescent agent DCM. The fluorescence signal appeared after 0.5 h and the intensity become stronger with time increasing, indicative of cleavage of -S-S- bond between the GEM and DCM. Moreover, the fluorescence signal was still visualized after 24 h, suggestive of long-time tracing ability. That means, the nanomized prodrug DCM-S-GEM/PEG can long-time trace the drug release in biological environment. The fluorescence signal spreaded around the mice body in DCM-S-GEM treatment group after 4 h post injection, suggestive of poor tumor retention (Fig. 7A). Whereas, the fluorescence signal of the mice in DCM-S-GEM/PEG treatment group still remains in the tumor site, guaranteed of longer tumor retention time and possible stronger treatment effect (Fig. 7B) because the bigger size not easily to be push out according to the EPR effect.

The longer tumor retention ability of NIR nanomized prodrug DCM-S-GEM/PEG was also demonstrated by the *ex vivo* fluorescence images of main organs of lung xenograft tumor mice after

orthotropic injection of DCM-S-GEM and DCM-S-GEM/PEG for 24 h. As shown in Fig. 7, the fluorescence signal mainly appeared in liver and kidney rather than in tumor for DCM-S-GEM treatment group (Fig. 7C), compared with mainly in tumor for DCM-S-GEM/PEG treatment group (Fig. 7D). This phenomenon claimed the limited side effect of DCM-S-GEM/PEG compared with free DCM-S-GEM. These experiments demonstrated that the nanomized prodrug DCM-S-GEM/PEG is not only perfect for long-time and real-time tracing drug *in vivo*, but also improving the therapeutic efficiency.

Conclusions

We focused on how to micellize fluorescent prodrug for solving its bioavailability and tumor targeting ability. We exploited diblock polymer DSPE-mPEG to nanomize the tumor-microenvironment active NIR fluorescent prodrug DCM-S-GEM/PEG for avoiding fast metabolism, displaying longer tumor retention, and achieving precise drug release in lung tumor. It is well demonstrated that DCM-S-GEM/PEG exhibits higher photostability, excellent specificity and sensitivity towards GSH. Compared with the free prodrug DCM-S-GEM, the nanomized prodrug DCM-S-GEM/PEG exhibits better biocompatibility, faster cell endocytosis rate, and 8-fold higher fluorescence imaging in tumor cells, showing significant toxicity to A549 tumor cells owing to the improved better aqueous dispersity, higher biocompatibility, and more efficient tumor cell endocytosis. In addition, *in vivo* investigations demonstrate that DCM-S-GEM/PEG leads to longer retention time than the free small prodrug DCM-S-GEM in the tumor mice model due to the EPR effect. The longer retention time in tumor tissue can increase the accumulation and the subsequent cellular internalization, so as to realize better NIR fluorescence imaging and sufficient cleavage of prodrug, generating higher treatment efficiency. The nanomized tumor-microenvironment active NIR prodrug DCM-S-GEM/PEG provides a novel approach to realize real-time and long-time tracking the drug delivery and activation process without systemic toxicity *in vivo*.

Conflict of interest

There are no conflicts of interest to declare.

Acknowledgements

The authors acknowledge financial support from NSFC/China (21788102, 21421004, 21636002 and 81602718), National key Research and Development Program (2016YFA0200300), Fundamental Research Funds for the Central Universities (222201814013), Shanghai Health and Family Planning Commission Research Foundation (201540158), and Program of Introducing Talents of Discipline to Universities (B16017).

Notes and References

1 A. J. Breugom, M. Swets, J. F. Bosset, L. Collette, A. Sainato, L. Cionini, R. G. Jones, N. Counsell, E. Bastiaannet, C. B. M. Broek, G. J. Liefers, H. Putter and C. J. H. Velde, *Lancet Oncol.,* 2015, **16,** 200-207.
2 M. Markman, *Nat. Rev. Clin. Oncol.*, 2015, **12,** 628-630.
3 A. H. Schmidt, M. Høyer, B. F. S. Jensen and M. Agerbaek, *Acta Oncol.*, 2018, **57,** 1084-1093.
4 R. Mahato, W. Y. Tai and K. Cheng, *Adv. Drug Delivery Rev.*, 2011, **63,** 659-670.
5 M. Y. Peng, S. Y. Qin, H. Z. Jia, D. W. Zheng, L. Rong and X. Z. Zhang, *Nano Res.*, 2016, **9,** 663-673.
6 Y. Tsume, A. J. Drelich, D. E. Smith and G. L. Amidon, *Molecules*, 2017, **22,** 1322.
7 K. Sefah, D. H. Shangguan, X. L. Xiong, M. B. O'Donoghue and W. H. Tan, *Nat. Protoc.*, 2010, **5,** 1169-1185.
8 J. .S Ross, C. E. Sheehan, H. A. Fisher, R. P. Jr Kaufman, P. Kaur, K. Gray, I. Webb, G. S. Gray, R. Mosher and B. V. Kallakury, *Clin. Cancer Res.*, 2003, **9,** 6357-6362.
9 L. Fang, R. F. Battisti, H. Cheng, P. Reigan, Y. Xin, J. Shen, D. Ross, K. K. Chan, E. W. Jr Martin, P. G. Wang and D. Sun, *J. Med. Chem.*, 2006, **49,** 6290-6297.
10 Y. Kang, X. Tang and Z. Cai, *Adv. Funct. Mater.*, 2016, **26,** 8920-8931.
11 S. Gnaim, A. Scomparin, S. Das, R. Blau, R. S. Fainaro and D. Shabat, *Angew. Chem. Int. Edit.*, 2018, **57,** 9033-9037.
12 M. H. Lee, J. Y. Kim, J. H. Han, S. Bhuniya, J. L. Sessler, C. Kang and J. S. Kim, *J. Am. Chem. Soc.*, 2012, **134,** 12668-12674.
13 H. Z. Chen, H. Jia, H. P. Tham, Q. Y. Qu, P. Y. Xing, J. Zhao, S. Z. F. Phua, G. Chen and Y. L. Zhao, *ACS Appl. Mater. Interfaces*, 2017, **9,** 23536-23543.
14 M. Y. Marzbali and A. Y. Khosroushahi, *Cancer Chemoth. Pharm.*, 2017, **79,** 637-649.
15 M. L. Pei, X. Jia, X. B. Zhao, J. G. Li and P. Liu, *Carbohyd. Polym.*, 2018, **183,** 131-139.
16 Z. S. Jia, X. B. Wang, X. Wei, G. Zhao, K. W. Foster, F. Qiu, Y. Y. Gao, F. Yuan, F. Yu, G. M. Thiele, T. K. Bronich, J. R. O'Dell and D. Wang, *ACS Nano*, 2018, **12,** 7663-7681.
17 Y. Jiang, X. Z. Wang, X. Liu, W. Lv, H. J. Zhang, M. W. Zhang, X. R. Li, H. L. Xin and Q. W. Xu, *ACS Appl. Mater. Interfaces*, 2017, **9,** 211-217.
18 J. Y. Li, L. Qiu, X. F. Xu, C. Y. Pan, C. Y. Hong and W. J. Zhang, *J. Mater. Chem. B*, 2018, **6,** 1678-1687
19 P. Thapa, M. Li, R. Karki, M. Bio, P. Rajaputra, G. Nkepang, S. Woo and Y. You, *ACS Omega*, 2017, **2,** 6349-6360.
20 F. Y. Zhou, B. Feng, T. T. Wang, D. G. Wang, Z. R. Cui, S. L. Wang, C. Y. Ding, Z. W. Zhang, J. Liu, H. J. Yu and Y. P. Li, *Adv. Funct. Mater.*, 2017, **27,** 1703674.
21 G. W. Lin, P. N. Manghnani, D. Mao, C. Teh, Y. H. Li, Z. J. Zhao, B. Liu and B. Z. Tang, *Adv. Funct. Mater.*, 2017, **27,** 1701418.
22 D. E. Barry, J. A. Kitchen, M. Albrecht, S. Faulkner, T. Gunnlaugsson, *Langmuir*, 2013, **29,** 11506-11515.
23 C. X. Yan, Z. Q. Guo, Y. Y. Shen, Y, Chen, H. Tian and W. H. Zhu, *Chem. Sci.*, 2018, **9,** 4959-4969.
24 K. Z. Gu, Y. S. Xu, H. Li, Z. Q. Guo, S. J. Zhu, S. Q. Zhu, P. Shi, T. D. James, H. Tian and W. H. Zhu, *J. Am. Chem. Soc.*, 2016, **138,** 5334-5340.
25 X. H. Wang, Z. Q. Guo, S. Q. Zhu, Y. J. Liu, P. Shi, H. Tian and W. H. Zhu, *J. Mater. Chem. B*, 2016, **4,** 4683-4689.
26 Y. Tang, A. D. Shao, J. Cao, H. Li, Q. Li, M. Y. Zeng, M. Liu, Y. S. Cheng and W. H. Zhu, *Sci. China Chem.*, 2018, **61,** 184-191.
27 X. M. Wu, X. Sun, Z. Q. Guo, J. B. Tang, Y. Shen, T. D. James, H. Tian and W. H. Zhu, *J. Am. Chem. Soc.*, 2014, **136,** 3579-3588.
28 F. Y. Wang, L. Zhou, C. C. Zhao, R. Wang, Q. Fei, S. H. Luo, Z. Q. Guo, H. Tian and W. H. Zhu, *Chem. Sci.*, 2015, **6,** 2584-2589.
29 H. Sies, *Free Radical Bio. Med.*, 1999, **27,** 916-921.
30 S. Maiti, N. Park, J. H. Han, H. M. Jeon, J. H. Lee, S. Bhuniya, C. Kang and J. S. Kim, *J. Am. Chem. Soc.*, 2013, **135,** 4567-4572.
31 D. Sobot, S. Mura, S. O. Yesylevskyy, L. Dalbin, F. Cayre, G. Bort, J. Mougin, D. Desmaële, S. Lepetre-Mouelhi, G. Pieters, B. Andreiuk, A. S. Klymchenko, J. L. Paul, C. Ramseyer and P. Couvreur, *Nat. Commun.*, 2017, **8,** 15678.
32 N. Thatcher, F. R. Hirsch, A. V. Luft, A. Szczesnad, T. E. Ciuleanu, M. Dediu, R. Ramlau, R. K. Galiulin, B. Bálint, G. Losonczy, A. Kazarnowicz, K. Park, C. Schumann, M. Reck, H. Depenbrock, S. Nanda, A. Kruljac-Letunic, R. Kurek, L. Paz-Ares and M. A. Socinsk, *Lancet Oncol.*, 2015, **16,** 763-774.

33 A. Arlt, A. Gehrz, S. Müerköster, J. Vorndamm, M. L. Kruse, U. R. Fölsch and H. Schäfer, *Oncogene*, 2003, **22,** 3243-3251.
34 F. Cappuzzo, T. Ciuleanu, L. Stelmakh, S. Cicenas, A. Szczésna, E. Juhász, E. Esteban, O. Molinier, W. Brugger, I. Melezínek, G. Klingelschmitt, B. Klughammer and G. Giaccone, *Lancet Oncol.*, 2010, **11,** 521-529.
35 J. J. Monsuez, J. C. Charniot, N. Vignat and J. Y. Artigoub, *Int. J. Cardiol.*, 2010, **144,** 3-15.
36 S. Hamada, A. Masamune, S. Miura, K. Satoh and T. Shimosegawa, *Cell. Signal.*, 2014, **26,** 179-185.
37 Y. J. Liu, S. J. Zhu, K. Z. Gu, Z. Q. Guo, X. Y. Huang, M. W. Wang, H. M. Amin, W. H. Zhu and P. Shi, *ACS Appl. Mater. Interfaces*, 2017, **9,** 29496-29504.
38 N. Zhao, B. Wu, X. Hu and D. Xing, *Biomaterials*, 2017, **141,** 40-49.
39 Y. Li, J. Y. Lin, H. J. Wu, M. M. Jia, C. H. Yuan, Y. Chang, Z. Q. Hou and L. Z. Dai, *J. Mater. Chem. B*, 2014, **2,** 6534-6548.
40 H. S. Jung, X. Q. Chen, J. S. Kim and J. Yoon, *Chem. Soc. Rev.*, 2013, **42,** 6019-6031.
41 J. D. Adams, B. H. Lauterburg and J. R. Mitchell, *J. Pharmacol. Exp. Ther.*, 1983, **227,** 749-754.
42 D. Y. K. Wong, Y. L. Hsiao, C. K. Poon, P. C. Kwan, S. Y. Chao, S. T. Chou and C. S. Yang, *Cancer Lett.*, 1994, **81,** 111-116.
43 C. C. Yeh, M. F. Hou, S. H. Wu, S. M. Tsai, S. K. Lin, L. A. Hou, H. Ma and L. Y. Tsai, *Cell Biochem. Funct.*, 2006, **24,** 555-559.
44 R. Mooney, A. A. Majid, J. Batalla, A. J. Annala and K. S. Aboody, *Adv. Drug Delivery Rev.*, 2007, **118,** 33-51.
45 S. Mura, D. T. Bui, P. Couvreur and J. Nicolas, *J. Control. Release*, 2015, **208,** 25-41.
46 Z. S. Zhao, X. D. Guo, S. Y. Li, G. Q. Yang, *Acta Chim. Sinica*, 2016, **74,** 593-596.
47 Q. Liu, M. Xu, T. S. Yang, B. Tian, X. L. Zhang and F. Y. Li, *ACS Appl. Mater. Interfaces*, 2018, **10,** 9883-9888.
48 L. Jiao, F. L. Song, B. Y. Zhang, H. F. Ning, J. N. Cui and X. J. Peng, *J. Mater. Chem. B*, 2017, **5,** 5278-5283.

View Article Online
DOI: 10.1039/C8TB03188F

Nanomized tumor-microenvironment active NIR fluorescent prodrug for ensuring synchronous occurrences of drug releasing and fluorescence tracing †

Qiang Li,[a] Jun Cao,[b] Qi Wang,*[,a] Jie Zhang,[a] Shiqin Zhu,[a] Zhiqian Guo[a] and Wei-Hong Zhu*[,a]

The nanomized NIR fluorescent prodrug for solving its bioavailability and tumor targeting ability. This nanomized tumor-microenvironment active NIR prodrug DCM-S-GEM/PEG provides a novel approach to realize real-time and long-time tracking the drug delivery and activation process without systemic toxicity *in vivo*.